Accepted Manuscript

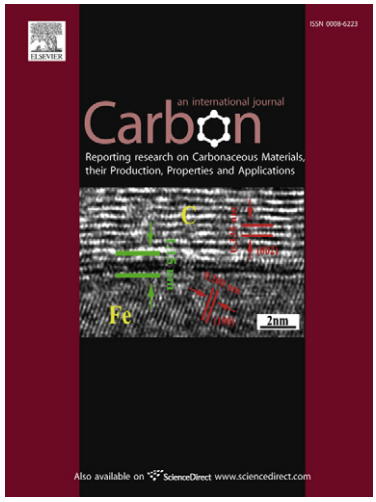

The spatial uniformity and electromechanical stability of transparent, conductive films of single walled nanotubes

Evelyn Doherty, Sukanta De, Philip E Lyons, Aleksey Shmeliov, Peter N. Nirmalraj, Vittorio Scardaci, Jerome Joimel, Werner J Blau, John J Boland, Jonathan N Coleman

PII: S0008-6223(09)00268-1
DOI: 10.1016/j.carbon.2009.04.040
Reference: CARBON 5323

To appear in: *Carbon*

Received Date: 21 November 2008
Accepted Date: 27 April 2009

Please cite this article as: Doherty, E., De, S., Lyons, P.E., Shmeliov, A., Nirmalraj, P.N., Scardaci, V., Joimel, J., Blau, W.J., Boland, J.J., Coleman, J.N., The spatial uniformity and electromechanical stability of transparent, conductive films of single walled nanotubes, *Carbon* (2009), doi: 10.1016/j.carbon.2009.04.040

The spatial uniformity and electromechanical stability of transparent, conductive films of single walled nanotubes

Evelyn Doherty[1,2], Sukanta De[1,2], Philip E Lyons[1,2], Aleksey Shmeliov[1], Peter N. Nirmalraj[2,3], Vittorio Scardaci[2,4], Jerome Joimel[2,4], Werner J Blau[1,2], John J Boland[2,3] and Jonathan N Coleman[1,2*]

[1]*School of Physics, Trinity College Dublin, Dublin 2, Ireland*

[2]*Centre for Research on Adaptive Nanostructures and Nanodevices, Trinity College Dublin, Dublin 2, Ireland*

[3]*School of Chemistry, Trinity College Dublin, Dublin 2, Ireland*

[4]*Hewlett Packard DIMO, Liffey Park Technology Campus, Barnhall Road, Leixlip, Co Kildare, Ireland*

We have prepared thin films of arc discharge single walled nanotubes by vacuum filtration. For film thicknesses greater than 40 nm, the films are of high optical quality; the optical transmission varies by <2% over the film area when measured with a spatial resolution of 4μm. However, the films become spatially non-uniform for film thickness below 40nm. The in-plane DC conductivity correlates with the uniformity, increasing from ~3800 S/m for a 10nm thick film to ~2-2.5×10^5 S/m for films of thickness >40 nm. Conductive atomic force microscopy maps show reasonably uniform current flow out of the plane of the film. For all thicknesses, the optical transmittance scales with film thickness as expected for a thin conducting film with optical conductivity of 1.7×10^4 S/m (λ=550nm). For films with t>40 nm the ratio of DC to optical conductivity was σ_{DC}/σ_{p}=13.0, leading to values of

* Corresponding author. Fax: +353 1 6711759. E-mail address: colemaj@tcd.ie (J. N. Coleman)

transmittance and sheet resistance such as T=80% and R_s=110Ω for the t=40 nm film. Electromechanically, these films were very stable showing conductivity changes of <5% and <2% when cycled over 2000 times in compression and tension respectively.

1 Introduction

Thin, transparent, conducting films are used for electrode applications in devices from liquid crystal displays to organic light-emitting diodes (OLEDs) and solar cells.[1] The most common materials used in such applications are doped tin oxides, notably indium tin oxide (ITO). However, ITO suffers from two considerable drawbacks. Firstly, the price of indium has soared over the last decade. Secondly, future display technology is likely to require flexible electrodes for applications such as e-paper. ITO is completely unsuited for such applications due to its brittleness, which results in irreversible loss of conductivity at strains above ~1%[2, 3].

Thus, it is clear that an ITO substitute is needed, preferably a material whose conductivity is invariant under flexing. To meet minimum industry standards, such a material should have a sheet resistance, $R_s \leq 100\ \Omega$ coupled with an optical transparency of $T \geq 90\%$ (λ=550 nm). This requires a material with relatively high conductivity and yet low optical absorbance as manifested by a large ratio of DC to optical conductivity, σ_{DC}/σ_{Op} (optical conductivity is related to the optical absorption co-efficient)[4]. It can be shown that industry targets can only be met for a material with $\sigma_{DC}/\sigma_{Op} \geq 35$. The search for such a material has been on-going for a number of years with thin films of carbon nanotubes being the main candidate.

Comprehensive measurements of transmittance and sheet resistance for thin nanotube films have been on-going for over 4 years. Early measurements showed σ_{DC}/σ_{Op}~1.[4] However, film quality has improved very rapidly with a number of groups contributing in the race to better films[5-17]. In recent years, the best results (high σ_{DC}/σ_{Op}) appear to come from films made from arc-discharge SWNTs[9, 10, 16, 18-20]. Currently, the best reported as-prepared films have values of σ_{DC}/σ_{Op}~13-16 for films prepared by spray coating home made arc discharge single walled nanotubes onto glass substrates[18]. Recently, Geng et al, reported spray coated films of pristine, commercially available, arc discharge SWNTs (Iljin Nanotech)

with σ_{DC}/σ_{Op}=10.1[10, 21]. These Iljin nanotech SWNTs appear to give the best results (for commercially available tubes) both for nanotube films and composites[22, 23]. More importantly, these Iljin films could be acid post-treated to give σ_{DC}/σ_{Op}=25.[10, 21] While acid treatment may result in the presence of mobile counter-ions[24], to the detriment of organic devices, this work shows that the industry goal of $\sigma_{DC}/\sigma_{Op}\geq$35 is probably attainable. Thus, this area of research has proceeded to the point where a number of important technical points must be answered. For example, when used as electrodes for organic light emitting diodes, it is not clear how spatially uniform these films are in terms of optical transmission, local nanotube density or current injection on the nanoscale. In addition, previous work has shown the film conductivity to drop for film thickness below 40 nm[10]. However, the nature of the fall-off warrants further study. In addition, while thin transparent nanotube films have been shown to be reasonably electrically stable under bending[20, 25], comprehensive bend and cycling tests have not been carried out.

In this paper we address these problems. We show that the fall off in conductivity at lower film thickness can be correlated with increases in film non-uniformity as measured by spatially resolved optical absorbance. At thicknesses >40nm the non-uniformity becomes thickness invariant, resulting in films with DC conductivity ~2.3×10^5S/m. These films have σ_{DC}/σ_{Op}=13.0 leading to values of T=80% and R_s=110 Ω for a 40 nm thick film. Electromechanical tests show the film conductivity to be extremely stable, changing by only a few percent over 2000 bend / release cycles.

2 Experimental procedure

Stock solutions of sodiumdodecylsulphate (SDS), sodium dodecylbenzenesulfonate (SDBS), lithiumdodecylsulphate (LDS), Sodium Cholate (SC) and Triton-X100, (all from Aldrich) of concentration 5mg/ml in millipore water, were prepared by overnight stirring.

These solutions were used to make stock nanotube dispersions by adding arc-discharge SWNTs (Iljin Nanotech, www.iljinnanotech.co.kr) such that the surfactant:SWNT mass ratio was 5:1 (nanotube concentration, 1 mg/mL). Each dispersion was subjected to 5 min of high-power tip sonication (VibraCell CVX; 750W, 20% 60 kHz), then placed in a sonic bath (Model Ney Ultrasonic) for 1 h, and then subjected to another 5 min of high-power sonication. They were then allowed to rest overnight before being centrifuged at 5500rpm for 90mins. The supernatant was carefully decanted and saved. The post-centrifuge nanotube concentration was determined from absorbance measurements (Cary 6000i). The supernatant was diluted with stock surfactant solution to give a final nanotube concentration of 0.005 mg/ml. Nanotube films were prepared by vacuum filtration of the above dispersions (0.005 mg/ml) using porous mixed cellulose ester filter membranes (MF-Millipore Membrane, mixed cellulose esters, Hydrophilic, 0.025 µm, 47 mm). The deposited films were washed with 200ml of millipore water followed by a wet transfer to a Polyethylene terephthalate (PET) substrate using heat and pressure[15]. The cellulose filter membrane was then removed by treatment with acetone vapour and subsequent acetone liquid baths followed by a methanol bath[15]. The film area was 36 mm in diameter. The film thickness, t, was calculated from the deposited mass per unit area, M/A, using $M/A=\rho t$, where ρ is the film density. While the density is not known for these films, a recent survey[26] of films made from a range of nanotube types shows the vast majority to have densities between 450 and 700 kg/m^3 (nanotube networks tend to be very porous). Thus we take the density as 570±150 kg/m^3, accepting this will result in a ~25% error in the nominal thickness and any dependant quantities such as DC or optical conductivity. In this study the film thickness ranges from ~10nm to ~100nm in thickness.

Transmission scans were made using an Epson Perfection V700 Photo flat-bed, white light, transmission scanner with a bit depth of 48 bits per pixel and a spatial resolution of 6400

dpi. The numerical output of the scanner was calibrated by scanning a range of neutral density filters. The resultant calibration curve was used to transform the output to represent transmittance. This results in a transmittance map with a transmittance value for every pixel. In some cases the transmittance was transformed to absorbance on a pixel by pixel basis using $A = -\log T$. The mean and standard deviation of the transmittance / absorbance were calculated from the entire data set ie from the entire set of transmittance / absorbance per pixel values. Scanning electron microscopy measurements were made using a Hitachi S-4300 Field Emission scanning electron microscope. Charging was avoided by transferring the nanotube film from cellulose membrane to a glass substrate coated with a thin palladium film. Atomic force microscope images were obtained using a Dimension V AFM. In order to extract the topography and conductance data simultaneously the microscope was operated in the conductance imaging mode (C-AFM). In this technique the AFM tip acts like a mobile probe on the surface and is held at ground potential and a DC bias is applied to the sample. The z feedback signal is used to generate a normal contact mode AFM topographic profile and the current passing between the tip and the sample is measured using a preamplifier to generate the conductance image. A bias voltage of 0.2mV up to 1V is applied to the electrode on the surface that drives current through the tubes. A current range of 2pA to 1μA can be detected by the preamplifier in the CI-AFM module. For this purpose a Cr/Pt coated conductive tip with a force constant of 3N/m and a resonant frequency of 75 kHz was employed. In all cases, the loading force employed during measurement was approximately 15nN. (The tips were purchased from Budget Sensors, ElectriMulti 75). Optical transmission spectra were recorded using a Cary Varian 6000i, with a sheet of PET used as the reference. Sheet resistance measurements were made using the four probe technique with silver electrodes of dimensions and spacings typically of ~mm in size and a Keithley 2400 source meter. Electromechanical measurements were made using a Zwick Z0.5 Proline tensile tester. The nanotube film on PET was bent into a semicircle which was constrained by the grips of the tensile tester. The film

was connected via two electrodes (attached to the grips) to a Keithley KE 2601. The bend radius was then defined by the distance between the grips. The inter-grip distance was then oscillated between typically 15mm and 5mm over many cycles. LabVIEW software recorded film resistance, inter-grip distance and cycle number.

3 Results and Discussion

Before carrying out detailed measurements on thin films of carbon nanotubes, we felt it necessary to test the dependence of film electrical properties on the surfactant used to disperse the nanotubes prior to film formation. As the surfactant used affects the quality of nanotube dispersion, namely the bundle diameter distribution[27], and the film conductivity is known to depend strongly on the mean bundle diameter[12, 26], we expect surfactant choice to influence the final film conductivity. Thus we prepared films of 50 nm thickness from SWNTs dispersed using five common surfactants: (SDS, SDBS, LDS, SC, Triton-X100). We found the conductivities of these films to be (2.3×10^5, 2.1×10^5, 2.2×10^5, 1.9×10^5, 3.8×10^4 S/m) respectively. We suggest that the deviation of the Triton results is due to lower dispersion quality and hence a poorer quality film. Due to their popularity, we chose to focus on SDBS and SDS for the remainder of this work.

Shown in figure 1A and B are photographs of films of Iljin SWNT (SDS) with thicknesses of 40 and 80 nm respectively. The film quality is immediately apparent. To explore this in more detail we made transmission scans of the same films (figure 1C and D). These scans are effectively white light transmission maps of the films. We performed scans with a spatial resolution of 4 μm (6400 dpi). The spatially averaged white-light transmittances were 75% and 61% for the film 40 nm and 80 nm films respectively. The uniformity of these films is given by the standard deviation of the transmittance, calculated over the entire film area, which were 0.9% and 1.1% for the 40 nm and 80 nm film respectively. The ratios of standard deviation

transmission to mean transmission for these films were 1.2% and 1.8% respectively. The low value of this quantity indicates the very high quality and optical uniformity of these films.

In order to characterise the film morphology we carried out SEM on nanotube films as a function of thickness. This is important as nanotube film conductivities scale with bundle diameter and film density.[26] Representative images for the SDS based films are shown in figure 2A-C for films of 20, 40 and 80 nm thick. Such images are typical of SWNT networks and show a porous network. For all thicknesses, the mean bundle diameter was invariant at ~20nm. In addition it appears as if the 20 nm thick film is less uniform than the thicker films, a point we will discuss below.

We further characterised the film morphology using AFM and C-AFM. Shown in figure 2D is an AFM image of the surface of a 10nm thick film of Iljin SWNTs prepared from SDS. We emphasise that this is an average thickness, calculated from a deposited mass per unit area of 5.5 mg/m^2. As we shall see below, considerable variations in local thickness are observed in this low thickness regime. In any case, a network similar to that in figure 2A can clearly be seen. Shown in figure 2 E is a C-AFM current map of the area of the Iljin film shown in figure 2 D. The current map of the Iljin film is similar to the topographical map in figure 2D showing a network of SWNT bundles from which current can flow out of the plane of the film. This is important as it shows that current can be gathered uniformly from all areas of the surface of these films. This is a critical property for any material with potential for use as an electrode. Interestingly we sometimes see domains of aligned nanotube bundles (figure 2F). We hypothesise that the formation of these regions may reflect the presence of a nematic phase of bundles in the dispersion.

For both SDS and SDBS films, the transmission spectra (figure 1E) were relatively featureless, displaying a slight dip around 700 nm which we associate with the presence of S_{22} optical transitions. Sharp transitions associated with van Hove singularities are not observed, probably due to broadening associated with nanotube aggregation[28]. In all cases the

transmittance decreased with increasing thickness, while the spectral profile remained invariant. Shown in figure 3A is the transmittance, T, (λ=550 nm) as a function of film thickness, t. For both film types, T falls from ~95% for 10nm thick films to ~60% for 100nm thick films, with all data falling on the same line. By modelling the interaction of thin conducting films (t<<λ) with light, it has been shown that the transmittance is related to the film thickness by[4, 29]

$$T(\lambda) = \left(1 + \frac{Z_0}{2}\sigma_{Op}(\lambda)t\right)^{-2} \qquad \text{Equation 1}$$

where Z_0 is the impedance of free space (377 Ω and σ_{Op} is the optical conductivity. This expression has been fitted to the data in figure 3A as shown by the dotted line. This curve fits both data sets well giving σ_{Op}=1.7±0.4×10^4 S/m (λ=550 nm), reasonably close to previously measured values of ~1.5×10^4 S/m for thin films of both Iljin SWNTs[21] and laser produced SWNT[30]. This agreement shows that our thickness calculation is reasonably accurate.

The measured sheet resistance for both surfactant types is shown in figure 3B as a function of film thickness, varying from ~3kΩ for t=10nm to 50-70 Ω for t=100nm. It is immediately clear that the SDS based films are slightly less resistive than the SDBS based films. As shown by the dotted lines, both data sets scale well as $R_s = 1/c_{DC}t$ for t>40 nm, suggesting the film morphology becomes thickness-invariant above this thickness. The DC conductivity is shown in figure 3C as a function of thickness. In line with the sheet resistance data, the conductivity is reasonably constant at higher values, but falls off below t=40nm. The thicker films have conductivities (t>40nm) of σ_{DC}≈1.9±0.5×10^{5}S/m and σ_{DC}≈2.3±0.5×10^{5}S/m for SDBS and SDS based films respectively. These conductivities are exceptionally high. The state-of-the-art for thin (un-doped) nanotube films is σ_{DC}≈1.5×10^{5}S/m which was measured for spray cast networks of Iljin SWNTs[21]. We speculate that the high conductivity of these films is due to the length of these Iljin SWNTs. We performed AFM measurements on sparse deposited networks. This

allowed the measurement of bundle lengths. We measured lengths between 1 and 10 microns with a mean and standard deviation of 3.5μm and 2 μm respectively. For comparison purposes, we carried out the same measurements for sparse networks of Hipco SWNTs prepared under similar conditions, measuring a mean and standard deviation of 0.8 μm and 0.4 μm respectively. As the conductivity of the nanotube films is expected to scale with bundle length[12], L, as $c \propto L^{1.7}$, we believe the length of these tubes to be an important factor contributing to the high conductivity of these films.

A number of recent papers have found a fall-off in conductivity at low thickness, similar to that observed here[10]. In very thin films, this can be attributed to percolation effects[4]. We propose that a network above the percolation threshold can be characterised by non-uniformities in areal nanotube density when measured on length scales similar to the mean nanotube length. We can explore this effect in more detail by measuring the local non-uniformity of the films as a function of thickness. We do this by recording transmission scans (pixel size 4 μm) of a number of the films discussed above. We transform the resulting transmission maps into absorbance (A) maps using $A = -\log T$. By the Lambert Beer law, the absorbance is proportional to the number of absorbing objects per unit area. This means the absorbance map is a measure of the spatial distribution of nanotubes per 4 μm pixel. For our purposes, we define the non-uniformity as the standard deviation of absorbance as measured over a 2mm×2mm grid (500×500 pixels). We associate a large degree of non-uniformity with a high standard deviation. We plot the data for non-uniformity versus sample thickness in figure 3D. It is clear from this data that the non-uniformity is constant for thicker films but increases sharply for films thinner than 40nm. This increase in non-uniformity correlates almost exactly with the thickness below which the conductivity falls off. Thus, we can observe a percolated network becoming bulk-like by measuring when the uniformity becomes invariant with thickness.

We have investigated the uniformity of these nanotubes films using spatially resolved transmission/absorbance measurements. However, we note that our results apply only to the type of films studied in this work ie those produced by vacuum filtration. A number of different techniques have been successfully demonstrated to produce nanotube films including spraying, spin coating, dip coating. It is likely that each of these techniques results in different degrees of uniformity. We emphasise that the results presented in this work only apply to vacuum filtered films. We are currently working to compare the spatial uniformity of vacuum filtered and spray cast films.

Shown in figure 4 is the transmittance (λ=550nm) plotted as a function of sheet resistance for both SDS and SDBS based films. For thin conducting films, T is related to R_s (in Ohms) by[4]

$$T(\lambda) = \left(1 + \frac{Z_0}{2R_s}\frac{\sigma_{Op}(\lambda)}{\sigma_{DC}}\right)^{-2} \qquad \text{Equation 2}$$

This model assumes constant values of σ_{DC} and σ_{Op}, such that both T and R_s vary as the film thickness is varied. This equation has been fitted to the data for both film types as shown by the dashed lines. In the inset the data is re-plotted such that data following equation 2 should follow a straight line, with the data showing good linearity. The fits give values of the conductivity ratio to be σ_{DC}/σ_{Op}=13.0 and σ_{DC}/σ_{Op}=10.5, reasonably consistent with the values for σ_{DC} and σ_{Op} calculated previously. These conductivity ratios are quite high. To the authors' knowledge, the state-of-the-art T, R_s data for as-prepared nanotube films, such as those presented here, results in σ_{DC}/σ_{Op}=13-16[18]. The best results for as-prepared films produced from commercially available nanotubes have been for films of Iljin SWNTs, giving σ_{DC}/σ_{Op}=10.1[21]. Thus our SDS data is slightly ahead of the state-of-the-art for as-prepared films of commercially available SWNTs.

However, as mentioned above, industry requires $R_s \leq 100\Omega$ coupled with $T \geq 90\%$ (λ=550 nm) for a material to qualify as an ITO replacement. Using equation 2, this means $\sigma_{DC}/\sigma_{op} \geq 35$. As σ_{op} is more or less fixed in these films, this means we need to increase σ_{DC} by a factor of ×2-2.5 to ~5×10^5 S/m to meet industry requirements. We note that the state-of-the-art as-prepared samples described above were improved by ×2.5 by acid post-treatment, resulting in σ_{DC}/σ_{op}=26. However, this technique is problematic if the nanotube films are to be used as electrodes in OLEDs or organic solar cells, as the presence of small mobile counter ions may poison the active layer. We believe a non chemical method is required to increase σ_{DC}/σ_{op}. There are two possibilities. The first is to prepare high volume fraction polymer-nanotube composite films using conducting polymer matrices. Such materials have recently been demonstrated, showing reduced σ_{op} resulting in increased σ_{DC}/σ_{op}[23]. Secondly, exfoliation of the nanotubes followed by film formation in such a way as to frustrate nanotube re-aggregation would result in films with smaller bundles. It has recently been suggested that the conductivity scales as D^{-3}.[26] Thus, a decrease in bundle diameter by only a factor of ×0.7 to ~15 nm would be enough to increase σ_{DC}/σ_{op} by ×2.8.

As mentioned above, these films have optical and electrical properties close to what is required to replace ITO. However, they are potentially even more useful as a *flexible,* transparent, electrode material. Such a material is of considerable interest as an electrode in applications such as e-paper. To test this, we prepared Iljin SWNT films on PET, made from SDS and SDBS at a number of thicknesses. In addition we prepared a 60 nm thick ITO film for comparison. In each case we monitored the sheet resistance during bending with the nanotube film both in tension and in compression. The films were bent from an initial radius of curvature of 7.5 mm to a final radius of 2.5 mm before being relaxed. Shown in figure 5A is the sheet

resistance versus radius of curvature during both the bending and release phase (note that the magnitude of the average strain felt by the film is plotted in the top axis[31]). As expected[2, 3], ITO fails catastrophically on tensile bending, with the sheet resistance increasing irreversibly by almost two orders of magnitude. In comparison, the sheet resistance of the SDS-based Iljin films (figures 5B-E) vary by <1% during both bend and release phases for films both in tension and compression. In contrast, while the SDBS film was very stable in tension, its sheet resistance varied significantly while bending in compression.

While these nanotube films are clearly relatively stable during one bend cycle, it is important to ascertain their stability over many bend cycles. Shown in figure 5F-J is the mean sheet resistance per cycle plotted versus cycle number for the same films examined in figure 5A-E. In figure 5F, we show cyclic test data for an ITO/PET film in the inset. In this case to avoid immediate failure, the film was tested at much lower curvature with minimum bend radius on each cycle of only 20 mm. The sheet resistance of this film increased by a factor of ×8 before failing around cycle 150. In contrast, the sheet resistance of the SDS-Iljin films fell by <5% in compression and <2% in tension over ~2000 cycles. The SDBS-Iljin films were similarly stable in tension but underwent a decrease in R_s of ~8% when cycled in compression. Note that none of these nanotube films failed during these measurements. The number of cycles was limited by time constraints.

4 Conclusions

We have prepared thin, flexible nanotube films with DC conductivity surpassing the state of the art. Initial tests have shown that dispersing the nanotubes with the surfactant sodium dodecyl sulphate gives the most conductive films. We find that the optical transmittance of SDS-prepared films scales with thickness as expected for a thin metallic film. Data analysis gives a value for the optical conductivity (λ=550nm) of 1.7×10^4 S/m, similar to

previous measurements. For thicknesses above 40 nm, the in-plane conductivity is constant at ~2×10^5 S/m. However, below 40nm, the conductivity falls off rapidly. This behaviour correlates with measurements of the film non-uniformity which show films with t<40nm to be significantly less uniform. Conductive AFM measurements show the current flow out of the film to be very uniform on length scales greater than ~2μm. For films with t>40nm the ratio of DC to optical conductivity was σ_{DC}/σ_{Op}=13.0, leading to values of transmittance and sheet resistance such as T=80% and R_s=110 Ω for the t=40 nm film. We have characterised the electromechanical stability of our films by monitoring the sheet resistance during bending. We monitor sheet resistance during one bend-release cycle as a function of strain for films bent both in tension and in compression. In addition, we monitor the average resistance per cycle over many bend cycles. We find the resistance change to be very small over the first cycle and typically <5% and <2% over >2000 cycles for films bent in compression and tension respectively. We believe that these results show that, pending a factor of ×3 increase in conductivity, these materials are suitable for use as an ITO replacement material.

Acknowledgements

We acknowledge the Science Foundation Ireland funded collaboration (SFI grant 03/CE3/M406s1) between Trinity College Dublin, University College Cork and Hewlett Packard, Dublin Inkjet Manufacturing Operation which as allowed this work to take place.

Figures

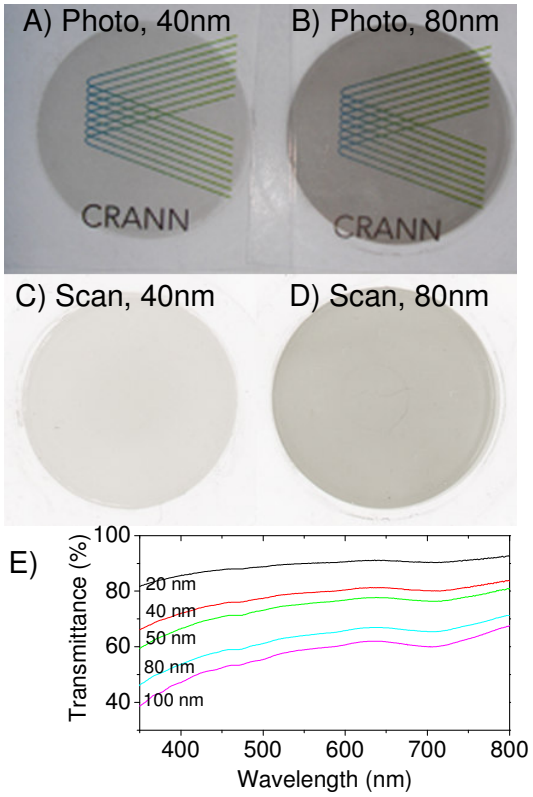

Figure 1 A) and B) Photographs of 40 and 80 nm thick Iljin SWNT (SDS) respectively. C) and D) Optical white-light transmission scans of the films pictured in A) and B). E) Transmission spectra for Iljin SWNT films (SDS) of thicknesses between 20 nm and 100 nm.

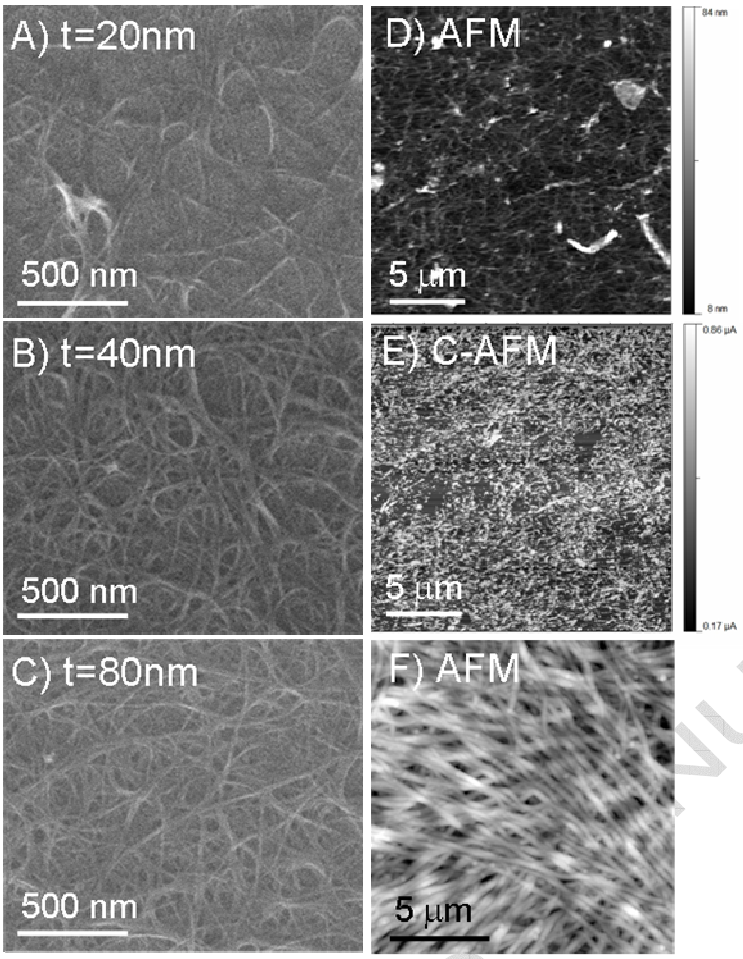

Figure 2 A-C) SEM images of selected nanotube films of various film thickness. D) An AFM image of the surface of a 10 nm thick Iljin/SDS film. E) A conducting-AFM image of the same region pictured in D). F) An AFM image of an aligned region of a 50nm thick Iljin/SDS film.

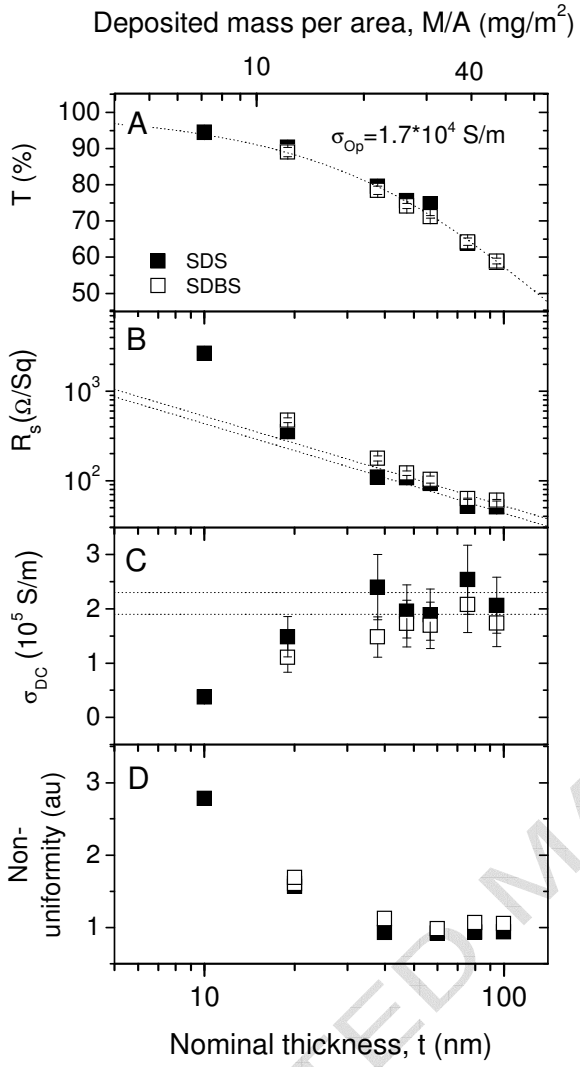

Figure 3 Properties of nanotube films as a function of film thickness, t, for both SDS and SDBS films. A) Optical transmittance, measured at 550 nm. The dotted line is a fit to equation 1, consistent with an optical conductivity of 1.7×10^4 S/m. B) Sheet resistance. The dotted lines are fits to $R_s = 1/(\sigma_{DC} t)$, where σ_{DC} is the DC conductivity. The upper and lower curves are consistent with DC conductivities of 1.9×10^5 S/m and 2.3×10^5 S/m respectively. C) DC conductivity, calculated from $R_s = 1/(\sigma_{DC} t)$. The upper and lower dotted lines illustrate DC conductivities of 2.3×10^5 S/m and 1.9×10^5 S/m respectively. D) Film non-uniformity as

defined by the standard deviation of local absorbance measured with a spatial resolution of 4 μm (scan area 2mm×2mm).

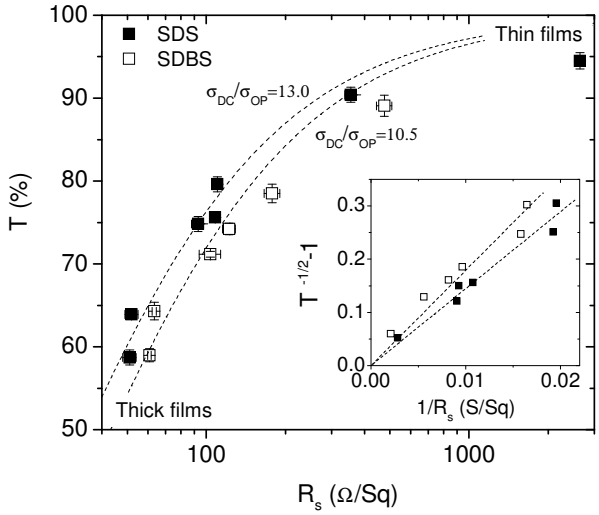

Figure 4 Transparency as a function of sheet resistance for both SDS and SDBS films. The dotted lines are fits to equation 2, consistent with σ_{DC}/σ_{Op} values of 13.0 and 10.5 for SDS and SDBS based films respectively. Inset: Transparency-sheet resistance data plotted to highlight the applicability of equation 2.

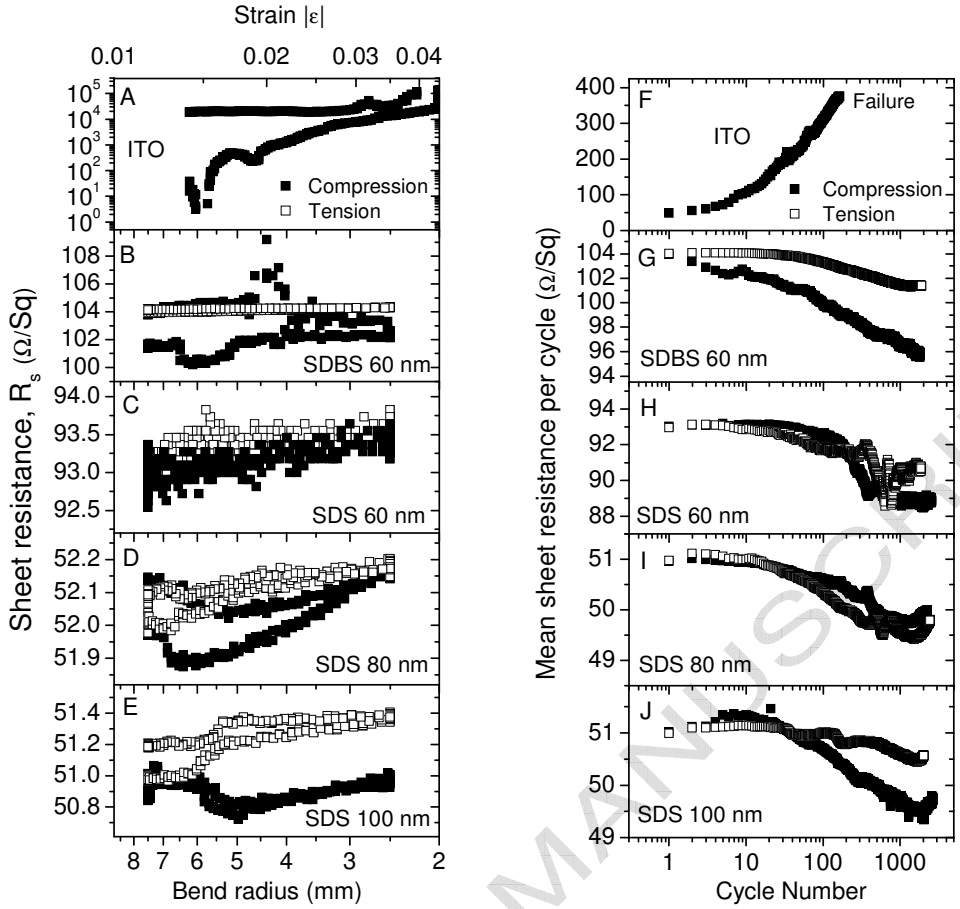

Figure 5 Data showing the electromechanical stability of nanotube films. A-E) Sheet resistance of films of ITO and nanotubes (prepared from SDBS and SDS of different thicknesses) during a bend cycle where the bend radius is reduced from 7.5 mm to 2.5 mm before relaxing back to 7.5 mm. Shown on the top axis is the strain associated with these bend radii. The ITO sample was measured in compression only, while the nanotube samples were measured both in tension and compression. Note that ITO fails completely under these conditions with R_s remaining at ~3×10^4 Ω when the sample was released (upper portion of curve). In contrast, the sheet resistance of the nanotube films vary by no more than 5%. F-J) Average sheet resistance per cycle for films identical to those in A-E) as a function of cycle number. For the nanotube films, each cycle was a bend-relaxation cycle as described above. However, to avoid failure on the first cycle, the ITO film was only bent to a radius of 20 mm. Note that while the ITO film

failed after 160 cycles, the nanotube films were not observed to fail. Rather, the number of cycles was limited by time constraints.

References

[1] Watcharotone S, Dikin DA, Stankovich S, Piner R, Jung I, Dommett GHB, et al. Graphene-silica composite thin films as transparent conductors. Nano Letters. 2007;7:1888-92.
[2] Leterrier Y, Medico L, Demarco F, Manson JAE, Betz U, Escola MF, et al. Mechanical integrity of transparent conductive oxide films for flexible polymer-based displays. Thin Solid Films. 2004;460:156-66.
[3] Chen Z, Cotterell B, Wang W. The fracture of brittle thin films on compliant substrates in flexible displays. Engineering Fracture Mechanics. 2002;69:597-603.
[4] Hu L, Hecht DS, Gruner G. Percolation in transparent and conducting carbon nanotube networks. Nano Letters. 2004;4:2513-7.
[5] Aguirre CM, Auvray S, Pigeon S, Izquierdo R, Desjardins P, Martel R. Carbon nanotube sheets as electrodes in organic light-emitting diodes. Applied Physics Letters. 2006;88:183104.
[6] Barnes TM, Wu X, Zhou J, Duda A, van de Lagemaat J, Coutts TJ, et al. Single-wall carbon nanotube networks as a transparent back contact in CdTe solar cells. Applied Physics Letters. 2007;90:243503.
[7] Contreras MA, Barnes T, van de Lagemaat J, Rumbles G, Coutts TJ, Weeks C, et al. Replacement of transparent conductive oxides by single-wall carbon nanotubes in Cu(In,Ga)Se-2-based solar cells. Journal of Physical Chemistry C. 2007;111:14045-8.
[8] Fanchini G, Unalan HE, Chhowalla M. Modification of transparent and conducting single wall carbon nanotube thin films via bromine functionalization. Applied Physics Letters. 2007;90:092114.
[9] Geng HZ, Kim KK, Lee K, Kim GY, Choi HK, Lee DS, et al. Dependence of material quality on performance of flexible transparent conducting films with single-walled carbon nanotubes. Nano. 2007;2:157-67.
[10] Geng HZ, Kim KK, So KP, Lee YS, Chang Y, Lee YH. Effect of acid treatment on carbon nanotube-based flexible transparent conducting films. Journal of the American Chemical Society. 2007;129:7758-9.
[11] Gruner G. Carbon nanotube films for transparent and plastic electronics. Journal of Materials Chemistry. 2006;16:3533-9.
[12] Hecht D, Hu LB, Gruner G. Conductivity scaling with bundle length and diameter in single walled carbon nanotube networks. Applied Physics Letters. 2006;89:133112.
[13] Parekh BB, Fanchini G, Eda G, Chhowalla M. Improved conductivity of transparent single-wall carbon nanotube thin films via stable postdeposition functionalization. Applied Physics Letters. 2007;90:121913.
[14] Pasquier AD, Unalan HE, Kanwal A, Miller S, Chhowalla M. Conducting and transparent single-wall carbon nanotube electrodes for polymer-fullerene solar cells. Applied Physics Letters. 2005;87:203511
[15] Wu ZC, Chen ZH, Du X, Logan JM, Sippel J, Nikolou M, et al. Transparent, conductive carbon nanotube films. Science. 2004;305:1273-6.
[16] Yim JH, Kim YS, Koh KH, Lee S. Fabrication of transparent single wall carbon nanotube films with low sheet resistance. Journal of Vacuum Science & Technology B. 2008;26:851-5.

[17] Zhang DH, Ryu K, Liu XL, Polikarpov E, Ly J, Tompson ME, et al. Transparent, conductive, and flexible carbon nanotube films and their application in organic light-emitting diodes. Nano Letters. 2006;6:1880-6.
[18] Barnes TM, de Lagemaat JV, Levi D, Rumbles G, Coutts TJ, Weeks CL, et al. Optical characterization of highly conductive single-wall carbon-nanotube transparent electrodes. Physical Review B. 2007;75:235410.
[19] Li ZR, Kandel HR, Dervishi E, Saini V, Xu Y, Biris AR, et al. Comparative study on different carbon nanotube materials in terms of transparent conductive coatings. Langmuir. 2008;24:2655-62.
[20] Ng MHA, Hartadi LT, Tan H, Poa CHP. Efficient coating of transparent and conductive carbon nanotube thin films on plastic substrates. Nanotechnology. 2008;19:205703.
[21] Geng HZ, Lee DS, Kim KK, Han GH, Park HK, Lee YH. Absorption spectroscopy of surfactant-dispersed carbon nanotube film: Modulation of electronic structures. Chemical Physics Letters. 2008;455:275-8.
[22] Moon JS, Park JH, Lee TY, Kim YW, Yoo JB, Park CY, et al. Transparent conductive film based on carbon nanotubes and PEDOT composites. Diamond and Related Materials. 2005;14:1882-7.
[23] De S, Lyons PE, Sorrel S, Doherty EM, King PJ, Blau WJ, et al. Transparent, flexible, and highly conductive thin films based on polymer-nanotube composites ACS Nano. 2009;3:714-20.
[24] Zhou W, Vavro J, Guthy C, Winey KI, Fischer JE, Ericson LM, et al. Single wall carbon nanotube fibers extruded from super-acid suspensions: Preferred orientation, electrical and thermal transport. Journal of Applied Physics. 2004;95:649-55.
[25] Kaempgen M, Duesberg GS, Roth S. Transparent carbon nanotube coatings. Applied Surface Science. 2005;252:425-9.
[26] Lyons PE, De S, Blighe F, Nicolosi V, Pereira LPC, Ferreira MS, et al. The relationship between network morphology and conductivity in nanotube films. Journal of Applied Physics. 2008;104:044302.
[27] Sun Z, Nicolosi V, Rickard D, Bergin SD, Aherne D, Coleman JN. Quantitative evaluation of surfactant-stabilized single-walled carbon nanotubes: Dispersion quality and its correlation with zeta potential. Journal of Physical Chemistry C. 2008;112:10692-9.
[28] Reich S, Thomsen C, Ordejon P. Electronic band structure of isolated and bundled carbon nanotubes. Physical Review B. 2002;65:155411.
[29] Dressel M, Gruner G. Electrodynamics of Solids: Optical Properties of Electrons in Matter. Cambridge: Cambridge University Press 2002.
[30] Ruzicka B, Degiorgi L, Gaal R, Thien-Nga L, Bacsa R, Salvetat JP, et al. Optical and dc conductivity study of potassium-doped single-walled carbon nanotube films. Physical Review B. 2000;61:R2468-R71.
[31] Dikin DA, Stankovich S, Zimney EJ, Piner RD, Dommett GHB, Evmenenko G, et al. Preparation and characterization of graphene oxide paper. Nature. 2007;448:457-60.